Journal of King Saud University – Science 34 (2022) 101938

Contents lists available at ScienceDirect

Journal of King Saud University – Science

journal homepage: www.sciencedirect.com

Original article

Synthesis of zinc oxide based etoricoxib and montelukast nanoformulations and their evaluation through analgesic, anti-inflammatory, anti-pyretic and acute toxicity activities

Sulaiman Sulaiman [a,b], Shabir Ahmad [a], Syeda Sohaila Naz [b], Sara Qaisar [b], Sayyar Muhammad [a], Riaz Ullah [c,*], Mohammad Khalid Al-Sadoon [d], Aneela Gulnaz [e]

[a] Department of Chemistry, Islamia College University, Peshawar, KPK, Pakistan
[b] Nanosciences and Technology Department, National Centre for Physics, Quaid-i-Azam University Campus, Islamabad 44000, Pakistan
[c] Department of Pharmacognosy, College of Pharmacy, King Saud University, Riyadh, Saudi Arabia
[d] Department of Zoology, College of Science, King Saud University, PO Box 2455, Riyadh 11451, Saudi Arabia
[e] College of Pharmacy, Woosuk University, Wanju-gun 55338, Republic of Korea

ARTICLE INFO

Article history:
Received 8 November 2021
Revised 14 February 2022
Accepted 28 February 2022
Available online 4 March 2022

Keywords:
Zinc oxide nanoparticles
Etoricoxib
Montelukast
Analgesic activity
Anti-inflammatory activity
Anti pyretic activity

ABSTRACT

The current study described the synthesis of novel low dose PVA capped Etoricoxib (ET) and montelukast (MT) conjugated Zinc Oxide (ZnO) nanomaterials (NMs) as potential anti-inflammatory, analgesic and antipyretic agents. A facile coprecipitation protocol was used for synthesis of NMs by combination of ET, MT and ZnO NP. The efficient synthesis of ET and MT conjugated ZnO NMs were confirmed through UV–visible, XRD, FTIR and DLS analysis. Data of *in vivo* anti-inflammatory activity indicated that potency of ZnO NMs was found to be greater than drugs (ET and MT). Analgesic potency of NMs was much higher than that of drugs (ET and MT). The *in vivo* antipyretic activity indicates that the results of NMs and drugs (ET and MT) are of similar effect but that of NMs are more potent based on per weight basis. A wide therapeutic window was shown by the acute toxicity study carried out via LD50 method. It is concluded that the novel low dose PVA capped ET and MT conjugated ZnO NMs were potential analgesic, antipyretic and anti-inflammatory agents.

1. Introduction

The response of the body to injury, like tissue damage and repair, is inflammation (Kwiecien and McHugh, 2021; Vane and Botting, 1996). Pain, fever and inflammation can be usually demonstrated in patient of cancer (Walia and Thakur, 2021), arthritis (Gupta et al., 2021) and other infections (Harb et al., 2021). Nonsteroidal anti-inflammatory drugs (NSAIDs) are the most commonly prescribe drugs for the treatment of inflammation, fever and pain (Kaduševičius, 2021; Sinniah et al., 2021) during arthritis and cancer worldwide (Moore et al., 2015; Ullah et al 2019). The mechanism of action of NSAIDs is to inhibits cyclooxygenase (COX) which play vital role in the initiation of inflammation (Singh et al., 2021). Apart from COX, lipoxygenases (5-LOX) and leukotriene product are also responsible for initiation of inflammation in the body (Demirci et al., 2022; Liu et al., 2022). Phospholipase A2 catalysis conversion of phospholipids to Arachidonic acid (AA) (Crupi and Cuzzocrea, 2022; Zhou et al., 2021). Where conversion of AA to prostaglandin and leukotriene is catalysed by COX and 5-LOX respectively (Jiang et al., 2022; Sinha et al., 2013). There two form of COX that is COX-1 (responsible for protection of lining of stomach and production of thromboxane) and COX-2 (responsible for synthesis of prostaglandin which leads to inflammation). Most of the NSAIDs (e.g. Naproxen, Diclofenac, Ibuprofen, Paracetamol and Mefenamic acid etc) blocks both COX which leads to gastrointestinal (GI) problems (Domper Arnal et al., 2021; Hameed et al., 2020; El-Mekkawy et al 2020), therefore selective COX-2 inhibitors are vital (Díaz-González and Sánchez-Madrid, 2015; Sağlık et al., 2021). Although some selective COX-2 inhibitor NSAIDs (valdecoxib, Rofecoxib, Celecoxib, Parecoxib, ET) were synthesised but most of them (e.g. valdecoxib) were banned and

* Corresponding author.
E-mail address: rullah@ksu.edu.sa (R. Ullah).
Peer review under responsibility of King Saud University.

Production and hosting by Elsevier

https://doi.org/10.1016/j.jksus.2022.101938
1018-3647/

withdrawn from market by FDA due to their sever cardiovascular adverse effects (Pawlosky, 2013).

Although traditional NSAIDs and selective COX-2 inhibitors are prescribed commonly for the treatment of inflammation, pain and fever but their long term use leads to adverse side effects, and does not inhibits 5-LOX and other leukotriene products (Sinha et al., 2013). Therefore, an effort was made to synthesis PVA capped ET and MT conjugated ZnO NMs. ZnO nanoparticle (NPs) were used as nanocarrier of ET (selective COX-2 inhibitor) (Guvenal et al., 2021) and MT (leukotriene inhibitor). The properties of nanoscale materials (both physical and chemical properties) vary from bulk form (Syed et al., 2021; Syed et al., 2013), therefore the potency of the drugs is enhanced.

2. Experimental

2.1. Materials and instrumentation

Zinc nitrate hexahydrate ($Zn(NO_3)_2{\cdot}6H_2O$), sodium hydroxide (NaOH), ethanol, ET, poly ethylene glycol (PEG, 6000), polyvinyl acetate (PVA, 89–98,000, 99% hydrolysed) and MT were purchased from Merck. Ultraviolet–Visible (UV–Vis) spectra were recorded through UV–Vis spectrometer (Perkin Elmer, Lambda 25), at National Centre for Physics Islamabad, Pakistan. The Fourier transform infrared spectroscopy (FTIR) analysis was carried out at the range of 500–4000 cm^{-1} through JASCO FT/IR-6600 at National Centre for Physics Islamabad, Pakistan. FTIR is measuring the vibrations of atoms, molecules and functional group which corresponds to the matching frequency of the infrared beam. The X-Ray Diffraction (XRD) spectra were performed for investigation of crystallite size, miller indices and phase determination via D8 advance Bruker X-ray diffractometer (Bruker Germany) at National Centre for Physics Islamabad, Pakistan. The spectra were calculated in the range of 10–90 2θ. Zetasizer or Dynamic light scattering (DLS) was performed at Pharmacy Department, Quaid e Azam University Islamabad, Pakistan. The size, shape, texture and morphology of nanoparticles was investigated through Scanning Electron Microscopy (SEM) at PINSTIC Islamabad, Pakistan. The paw volume was measured through Plethysmometer (UGO BASILE 7140) at Department of Biochemistry, Quaid e Azam University, Islamabad Pakistan.

2.2. Synthesis of nanomaterials

2.2.1. Step 1. Synthesis of ZnO NPs

ZnO NPs were synthesised through coprecipitation method (Raoufi, 2013). $Zn(NO_3)_2{\cdot}6H_2O$ was used as precursor salt. $Zn(NO_3)_2{\cdot}6H_2O$ (Saravanan et al., 2018) was reduced through NaOH to prepare ZnO NPs (Romadhan et al., 2016). 100 mM solution of NaOH was added to 100 mM solution of $Zn(NO_3)_2{\cdot}6H_2O$ @4 drop per minute in the presence of PEG with constant stirring. The addition of NaOH was stopped when the pH was reached to 10. The mixture was heated at 60 oC for 30 min. The pH was maintained at 7 through washing with deionised water. Precipitate was collected via filtration process. Precipitate was got dried at 60 oC. The dried NPs were grinded and then calcinated at 500 oC for 4 h (Ghorbani et al., 2015; Luna and Commission, 2015).

2.2.2. Step 2. Synthesis of PVA capped ET and MT conjugated ZnO NMs

ZnO NPs were used as nanocarrier for the ET and MT (Fakhar-e-Alam et al., 2014; Xiong, 2013). Solutions of ZnO NPs, ET and MT were prepared in ethanol, which were sonicated for 1 h for complete dissolution. Xml of ZnO NPs was kept on constant stirring, and Yml of ET and Zml of MT were added to it @4 drop per minute as shown in the Table 1. The mixture was post stirred for 2 h and then post sonicated for 2 h. Drug loading efficiency was 75–80%. The drugs were loaded on ZnO NPs through adsorption principles (Gaihre et al., 2009). The NMs were isolated through centrifugation at 6000 rpm for 1 h, which were then dried at 60 °C. ZnO NMs were encapsulated with PVA @2.5%. The PVA capped ET and MT conjugated ZnO NMs (ZE1, ZE2, ZE3, ZE4, ZE5, ZE6 and ZE7) were dried at 60 °C.

2.2.3. Quantification protocol

The aim of the quantification protocol was to evaluate the quantity of ET and MT in the NMs. Therefore, the quantification was carried out through UV/Vis spectroscopy (Jat et al., 2010). This protocol was performed for separate as well as combined samples of drugs. The UV/Vis spectrum was run at the wavelength of 200–800 nm. The samples of drugs were prepared in ethanol. Different ratios of ET and MT were loaded on ZnO NPs. The spectra were run before and after loading on ZnO NPs and quantity of drugs was calculated. 10 mg of each drug and NMs were dissolved in 20 ml of ethanol in separate beakers. The samples were sonicated and centrifuged (6000 rpm) for one hour. The difference in the quantity of drugs, before and after loading on ZnO NPs, was calculated from the UV/Vis spectra (Prajapati et al., 2022).

2.3. Bioactivity testing

2.3.1. In vitro anti-inflammatory activity

The primary rout of inflammation is denaturing of proteins in the body (Chandra et al., 2012). Therefore, inhibition of denaturing of protein is of primary concern to stop inflammation. In this research work inhibition of denaturing of Bovine Serum Albumin (BSA) activity (Chandra et al., 2012) was performed to measure the potency of drugs (ET and MT) and NMs against inflammation (Bailey-Shaw et al., 2017). Egg albumen method is also used for i*n vitro* anti-inflammatory activity but during incubation the egg albumin may coagulate at high temperature which will affect the results (Fig. 1).

Therefore, 5 mg/ml solution of each ZnO NPs, Et, Mt and ZnO NMs (i.e. ZE1, ZE2, ZE3, ZE4, ZE5, ZE6 and ZE7) were prepared in Dimethyl sulfoxide (DMSO), while that of Diclofenac sodium was prepared in water as 2 mg/ml, and was used as standard. Then 0.9 ml of BSA solution (1% BSA in deionized water) was added to 0.1 ml solution of each sample. These solutions were incubated for 20 min at 37 °C and then again incubated for 20 min at 55 °C. And were evaluated with UV/Vis spectroscopy at 660 nm (Leelaprakash and Dass, 2011) (Fig. 2).

2.3.2. In vivo anti-inflammatory activity

This activity was performed in albino mice through carrageenan induced hind paw oedema method (Rahmawati et al., 2022). The mice were weighed, marked and grouped in different cages. Volume of paw of mice was measured through Plethysmometer (UGO BASILE 7140) before and after the treatment of carrageenan. Carrageenan induces swelling and inflammation in the body, therefore its inhibition is measured for evaluation of potency of a drug. 1% carrageenan solution was prepared in normal saline and its 0.1 ml was injected to left hind paw of each mouse. Doses of drugs (diclofenac sodium (positive control), ET and MT) were given @10 mg/kg body weight, and that of ZnO NMs were given @5 mg/kg body weight through intraperitoneal (i.p.) injection. Volume of paw was measured after each hour of treatment of doses for 3 h. Drug or NMs was not given to the negative control group but were only treated with normal saline (Moilanen et al., 2012; Ratheesh and Helen, 2007).

$$Percent\ inhibition = \frac{(V_{control} - - V_{test})}{V_{control}} \times 100$$

Table 1
Required quantities of ZnO, ET and MT.

S#	Code	ZnO (XmL)	ET (YmL)	MT (ZmL)
1.	ZE1	20	80	0
2.	ZE2	20	60	20
3.	ZE3	20	50	30
4.	ZE4	20	40	40
5.	ZE5	20	30	50
6.	ZE6	20	20	60
7.	ZE7	20	0	80

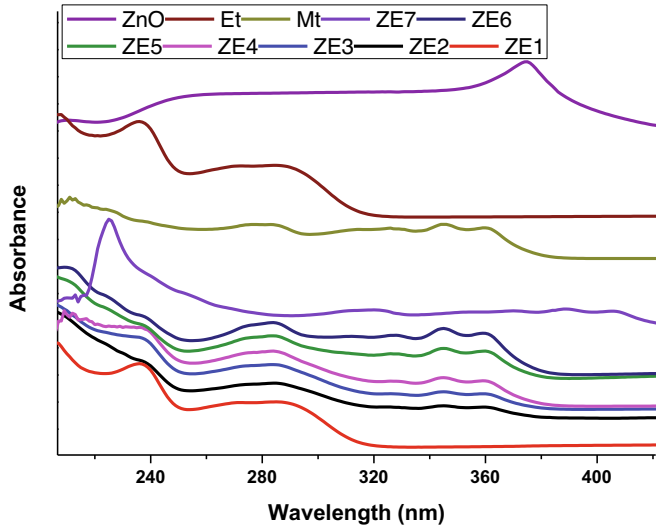

Fig. 1. UV/Vis spectrum of PVA capped ET and MT conjugated ZnO NMs.

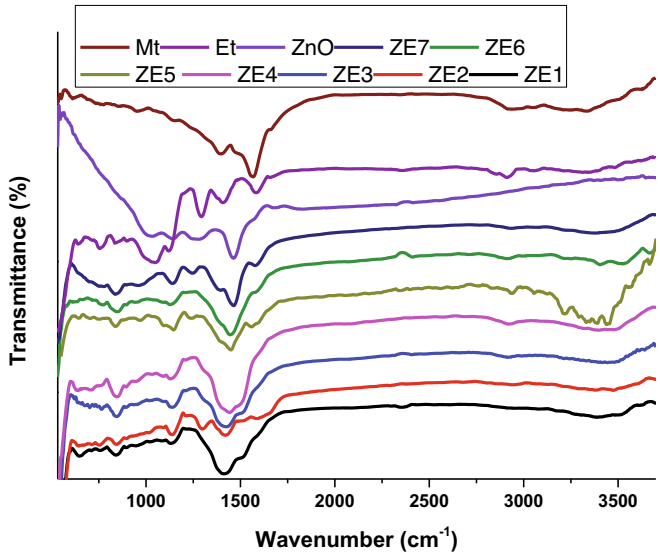

Fig. 2. FTIR spectrum of PVA capped ET and MT conjugated ZnO NMs.

2.3.3. In vivo analgesic activity

In vivo analgesic activity may be carried out through hot-plate method or acetic acid induced writhing method or both. Both methods are used for measurement of basic pain, with equal importance. In this research work, the *in vivo* analgesic activity was carried out through hot-plate method of Eddy and Leimbach (1953) in albino mice (O'Callaghan and Holtzman, 1975; Singh, 2022). Mice of both sexes were used in this activity. Average weight of mice was 26–28 g. Doses of drugs (diclofenac sodium (positive control), ET and MT) were given @10 mg/kg body weight, and that of ZnO NMs were given @5 mg/kg body weight through i. p. injection. Then each mouse was placed on hot plate at 55 °C for 30 s cut off time. The body movement of mice (i.e. jumping and paw licking) were keenly observed. This activity shows that if the NMs is more potent, then the mouse will takes more time on hot plate, and pain will be more inhibited and vice versa (Pathak and Argal, 2007).

2.3.4. In vivo anti pyretic activity

In vivo anti pyretic activity was performed through Brewer's yeast induced pyrexia method in albino mice (Estella et al., 2022; Hassan et al., 2015). A dose of 10 ml/kg of 20% aqueous brewer's yeast solution was injected to mice through subcutaneous to induce pyrexia (Makonnen et al., 2003). Body temperature of each mouse was measure through lubricated rectal thermometer before treatment of yeast solution. After 18 h body temperature of mice was measured again. Those mice were selected for this activity whose body temperature was increased by 0.6 °C. Doses of NMs and drugs were given through i.p. injection to each mouse. Body temperature of mice was measured for four hours after each hour (Abbah et al., 2010).

2.3.5. In vivo acute toxicity activity

In vivo acute toxicity activity was carried out in albino mice through the median lethal dose (LD50) method (Pohocha and Grampurohit, 2001; Zhang et al., 2022). Doses of NMs (5, 10, 20, 50, 100 and 200 mg/kg body weight) were given to mice through i.p. injection and were observed for 24 h after each dose. The purpose of this activity was to measure the maximum safe amount of NMs for organisms (Fig. 3).

2.4. Statistical analysis

The studied bioactivities data is expressed as standard error mean (SEM). The mean ± standard deviation (SD) was calculated for the data and then converted to SEM by the equation

$$\% \pm SEM = \frac{\% \pm SD}{\sqrt{3}}$$

3. Results and discussions

3.1. Structural analysis

3.1.1. UV–Visible analysis

Drugs (ET and MT), NMs and ZnO NPs were observed through UV/Vis spectroscopy at the range of 200–800 nm wavelength (λ). The peak at λ = 370 nm in the spectrum of ZnO is due to surface plasmon resonance (SPR) (Ghorbani et al., 2015; Janani et al., 2020). The characteristic SPR band of ZnO NPs was observed at 374 nm which has confirmed the synthesis of ZnO NPs (Patil and Taranath, 2016). Characteristic peak of ET was observed at 233 nm (Cacciari et al., 2020; Singh et al., 2012), while that of MT were observed at 284, 324, 343 and 360 nm (Saravanan et al., 2008). The characteristic peak of ZnO (i.e. at 374 nm) disappears in the ZnO NMs, which indicates the adsorption of the drugs (ET and MT). The characteristic peaks of ET and MT were prominent in those NMs where their concentration was higher. The presences of characteristics peaks of ET and MT indicate drug conjugation in ZnO NMs (Fig. 4).

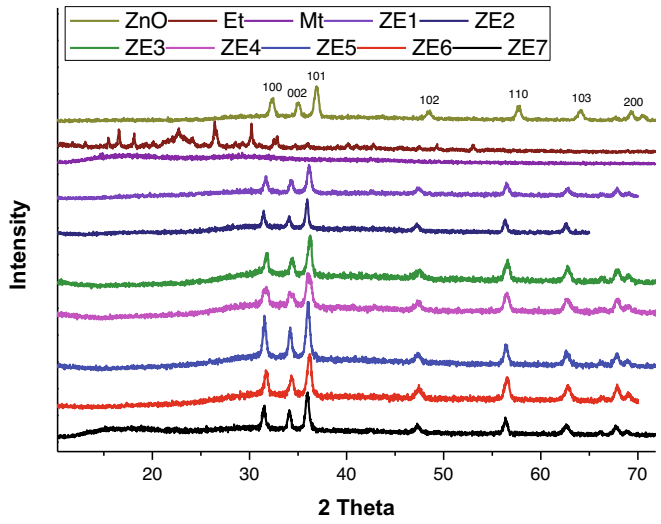

Fig. 3. XRD spectrum of PVA capped ET and MT conjugated ZnO NMs.

3.1.2. Fourier-transform infrared spectroscopy

The ZnO NPs, drugs and NMs were observed through FTIR spectroscopy at the range of 500–4000 cm^{-1}. The characteristic peak of ZnO NPs was detected at 555 cm^{-1} due to stretching vibrations of Zn–O bonds which indicates the hexagonal phase of ZnO NPs (Yedurkar et al., 2016). Characteristic peaks of Et were observed at 1010, 1140 (corresponding to sulphone groups (–S=O)) (Wahid et al., 2008), 1598.9 cm^{-1} (stretching vibration of C=N), 839.0, 781.1 and 638.0 cm^{-1} (stretching vibration of C–Cl) (Das et al., 2011; Kesharwani et al., 2016; Patel et al., 2007). The characteristic peaks of Mt were observed at 3396 (stretching of COOH), 2980 (aromatic stretching of C–H), 2925 (aliphatic stretching of C–H), 1610 (stretching of CC), 1595 (stretching of CN), 1497 (aliphatic bending of C–H), 1132 (stretching of C–O), 1068 (aromatic stretching of C–Cl), 837 (aromatic bending of C–H), 697 (stretching of C–S) (Priyanka and Hasan, 2012). The ZnO NMs follows the peak pattern of Et and Mt, which indicates conjugation with ZnO NPs. Although few of the peaks of Et and Mt were masked but most of them appears which shows their adsorption on ZnO NPs.

Table 2
Crystallite size of nanoformulations.

S. NO	Name	Crystallite size (nm)
1.	ZnO	19.73
2.	Et	41.64
3.	MT	Amorphous
4.	ZE1	22.41
5.	ZE2	32.15
6.	ZE3	20.45
7.	ZE4	17.30
8.	ZE5	21.38
9.	ZE6	18.90
10.	ZE7	21.42

3.1.3. X-Ray diffraction

The XRD pattern was studied at the range of 10–90 2θ for ZnO NPs, drugs (ET and MT) and NMs. The characteristic peaks of ZnO NPs were observed at 2 theta 32.5, 35.0, 36.9, 48.6, 57.7, 64.2 and 69.4 which were corresponding to 100, 002, 101, 102, 110, 103 and 200 planes of the Miller's indices of ZnO NPs, respectively (JCPDS data card NO 79-0207). The hexagonal structure of ZnO NPs was indicated from the XRD spectrum (Prabhu et al., 2013). Characteristic peaks of ET were observed in its XRD spectrum at 2θ = 11.9, 13.3, 16.5, 16.6, 18.2, 20.2, 22.8, 24.2, 26.5, 28.7, 29.4, 30.3, 32.5, 32.9, 34.8, 36.1, 39.1, 40.1, 41.2, 42, 42.9, 45.7, 47.6, 49.3 and 53.2 (Senthilkumar and Vijaya, 2015). These peaks were masked or disappeared in the NMs shows that ET was attached or converted to amorphous form. MT has no characteristic peak of XRD spectrum due its amorphous nature, but it has its specific pattern which was observed. The particle or crystallite size of drugs, NMs and NPs was calculate through Scherer's equation (Syed et al., 2022)

$$D = 0.9\lambda/\beta cos\theta$$

where D stands for crystallite size (Å), λ for wavelength of X-ray beam (1.54 Å), β for FWHM and θ is for Bragg's diffraction angle (Sharma et al., 2011).

3.1.4. DLS analysis of PVA capped ET and MT conjugated ZnO NMs

DLS was used for determination of size and zeta potential values of NPs. The size of particle was determined in suspension

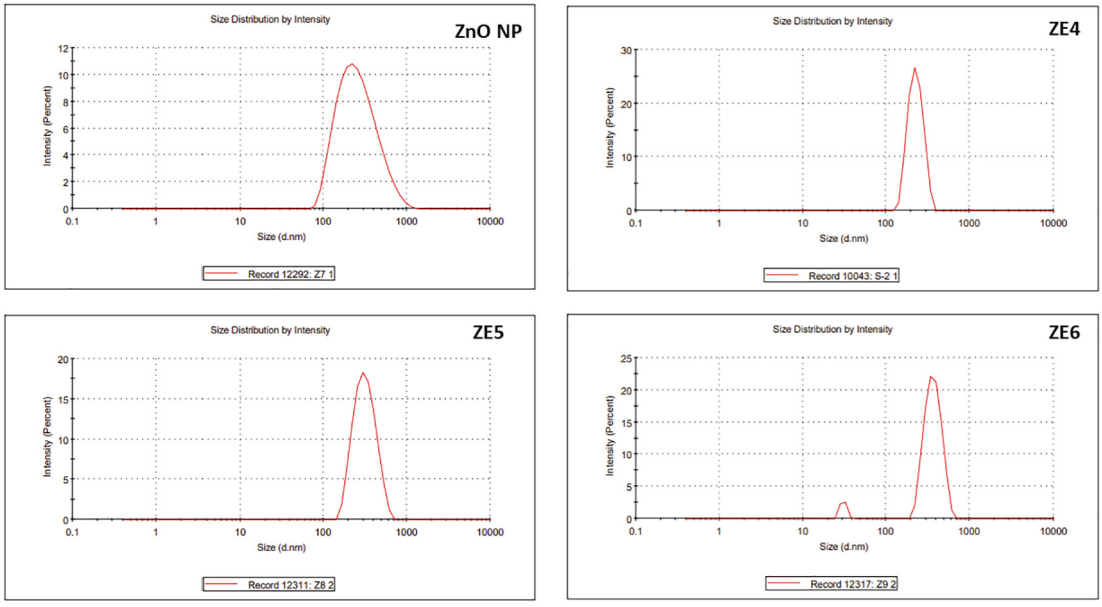

Fig. 4. DLS and Zeta potential spectra of ZnO NP, ZE4, ZE5 and ZE6.

Table 3
Quantity of ET and MT in 10 mg of ZnO NMs.

S. NO	5 mg	Etoricoxib (mg)	Montelukast (mg)	RSD (±)
1.	ZE1	5.6	–	0.06
2.	ZE2	4.3	1.3	0.08
3.	ZE3	3.7	1.41	0.07
4.	ZE4	2.89	2.69	0.08
5.	ZE5	1.53	3.6	0.07
6.	ZE6	1.49	4.2	0.05
7.	ZE7	–	5.92	0.06

Table 4
In vitro anti-inflammatory activity.

S. NO	Code	Absorbance at 660 nm	Inhibition (%) ± SEM
1.	Negative control (DMSO)	0.6900	0
2.	ZE1	0.3822	44.60 ± 1.18
3.	ZE2	0.3937	42.94 ± 1.53
4.	ZE3	0.3088	55.24 ± 1.36
5.	ZE4	0.147	78.69 ± 1.26
6.	ZE5	0.1093	84.15 ± 1.14
7.	ZE6	0.3822	83.57 ± 1.39
8.	ZE7	0.3937	72.46 ± 1.65
9.	ET	0.0221	96.80 ± 1.36
10.	MT	0.1476	78.61 ± 1.95
11.	ZnO	0.1557	77.43 ± 1.80
12.	Positive control (Diclofenac Sodium)	0.0755	89.06 ± 1.75

through this technique. The size of ZnO NPs, ZE4, ZE5 and ZE6 were 217, 285, 298 and 291 nm, respectively (Table 2).

3.1.5. Quantification of ET and MT

The quantity of ET and MT was investigated in ZnO NMs through UV/Vis analysis. The difference in the quantity of drugs, before and after loading on ZnO NPs, was calculated from the UV/Vis spectra. The wavelength for quantification of ET was 235 nm while for that of MT was 345 nm. But the best wavelength for both drugs was 282 nm. It was confirmed that the encapsulation efficiency (EE) was 70–75% Table 3, which was calculated through the following formula

$$EE\ \% = \frac{(Total\ drug\ added) - (non - entrapped\ drug)}{Total\ drug\ added} \times 100$$

3.1.6. In vitro anti-inflammatory activity

This activity is based on inhibition of denaturing of BSA, because denaturing of protein is the cause of inflammation. The % inhibition of denaturing of BSA was investigated through UV/Vis spectroscopy at 660 nm fixed wavelength. The % inhibitory effect was calculated through the following formula.

$$Percent\ inhibition = \frac{(Abs_{control} - - Abs_{test})}{Abs_{control}} \times 100$$

The denaturing of BSA was not inhibited in negative control, therefore inhibition of drugs and NMs was compared with it. Albeit the inhibitory effect of all the NMs was high but that of ZE4, ZE5 and ZE6 was very high. Therefore, these NMs were selected for further evaluation through *in vivo* studies. Results of % inhibition of denaturing of BSA through NMs is given in the Table 4 (Williams et al., 2008).

3.1.7. In vivo anti-inflammatory activity

In this activity mice were treated with NMs @ 5 mg/kg body weight, while dose of standards was given @10 mg/kg body weight. Mice were treated with 0.1 ml of carrageenan 1% solution through left hind paw to induce inflammation, which may also leads to swelling in the body. Therefore, the drugs and NMs were treated to inhibit it. The % inhibition of inflammation was estimated from the decrease in the volume of left hind paw of mice, which was measured through Plethysmometer (Azeem et al., 2010; Ilavarasan et al., 2006; Saleem et al., 2011). The following formula was used for calculation of % inhibition of inflammation.

$$Percent\ inhibition = \frac{(V_{control} - - V_{test})}{V_{control}} \times 100$$

The inhibition of inflammation was lower in first hour but increased in second and third hour. The % inhibitory effect of ZE6 was higher which is shown in the Table 5. On per weight base the inhibition of NMs was higher than free drugs (ET and MT).

3.1.8. In vivo analgesic activity

The hot plate method was used to evaluate albino mice for analgesic activity (delay in the latency of pain response) where they were treated with doses of drugs and NMs (ZE4, ZE5 and ZE6) through i.p. injections. Then, the animals were placed on hot plate at 55 ± 0.05 °C for 30 s cut off time to measure their tolerance against pain (Alvarenga et al., 2013). The body movements like jumping and licking of paws were keenly observed (Aziz et al., 2019). The time of tolerance on hot plate was noted which has indicated % pain inhibition. The % pain inhibition of ZE6 was very high as compared to other NMs which is shown in the Table 6. The analgesic potency of the NMs was higher than drugs (ET and MT) albeit the dose on per weight base was half of the drugs and standards.

3.1.9. In vivo anti pyretic activity

This activity was carried out in albino mice through Brewer's Yeast induced pyrexia method where the animals were treated with 20% Brewer's yeast @ 10 ml/kg body weight. Those mice were selected for activity whose body temperature was raised for 0.6 °C after 18 h of treatment of Brewer's yeast. The mice were then treated with doses of drugs (ET and MT) and NMs through i.p. injec-

Table 5
In vivo anti-inflammatory activity.

Drug	Dose (mg/kg)	Inhibitory effect (%) ± SEM		
		1 h	2 h	3 h
Negative control (Normal saline)	–	6.37 ± 1.08	4.75 ± 1.03	5.93 ± 1.02
Positive control (Diclofenac sodium)	10	68.84 ± 1.23	71.33 ± 1.12	85.78 ± 1.24
Et	10	65.19 ± 1.21	64.30 ± 1.53	79.26 ± 1.42
Mt	10	43.02 ± 1.24	48.10 ± 1.35	57.04 ± 1.45
ZE4	5	66.59 ± 1.24	62.16 ± 1.24	74.42 ± 1.24
ZE5	5	73.25 ± 1.24	75.00 ± 1.24	76.84 ± 1.24
ZE6	5	77.12 ± 1.24	60.30 ± 1.24	81.67 ± 1.24

Table 6
In vivo analgesic activity.

Drug	Dose (mg/kg)	Inhibitory effect (%) ± SEM		
		1 h	2 h	3 h
Negative control (Normal saline)	–	7.79 ± 1.02	6.20 ± 1.10	3.03 ± 1.21
Positive control (Diclofenac sodium)	10	58.34 ± 1.21	83.38 ± 1.24	83.22 ± 1.45
Et	10	24.30 ± 1.24	35.37 ± 1.10	48.61 ± 1.15
Mt	10 (Kolhe and Kale, 2017)	9.53 ± 1.32	7.95 ± 1.24	6.41 ± 1.42
ZE4	5	20.20 ± 1.11	36.28 ± 1.32	53.68 ± 1.55
ZE5	5	23.22 ± 1.21	30.22 ± 1.29	56.59 ± 1.65
ZE6	5	35.33 ± 1.39	57.04 ± 1.42	76.29 ± 1.43

Table 7
In vivo anti pyretic activity.

Drug	Dose (mg/kg)	Temperature (^{0}F)					
		Before yeast injection	0 h	1 h	2 h	3 h	4 h
Negative control (Normal saline)	–	98.6	101	101	101	101	101
Positive control (Paracetamol)	20 (Abbah et al., 2010)	98.6	100	98.6	98.6	98.6	98.6
Et	20	98.6	99.8	99	98.6	98.6	98.6
Mt	20 (Kolhe and Kale, 2017)	98.6	100.7	101	101	100.5	100.5
ZE4	5	98.6	101	99.4	99	98.6	98.6
ZE5	5	98.6	100.5	99	98.6	98.6	98.6
ZE6	5	98.6	101.4	98.6	98.6	98.6	98.6

tions. Body temperature was measure after each hour for 4 h through lubricated rectal thermometer. Body temperature of mice was controlled in the first hour by ZE4, ZE5 and ZE6 which is shown in the Table 7. It indicates the higher potency of NMs.

3.1.10. In vivo acute toxicity activity

This activity was carried out in albino mice through median lethal dose (LD50) method. Different doses of NMs were given to mice and were keenly monitored for a period of 24 h. The mice were natural up to a dose of 100 mg/kg body weight. But died when the dose was increased to 200 mg/kg body weight. It was confirmed that the NMs were acute toxic at or above 200 mg/kg body weight (Parra et al., 2001). According to the results of LD50 method of *in vivo* acute toxicity activity, these NMs were placed in category 3.

4. Conclusion

It is concluded that the novel low dose PVA capped ET and MT conjugated ZnO NMs were potential analgesic, antipyretic and anti-inflammatory agents. Data of the in vitro anti-inflammatory activity indicates that ZE4, ZE5 and ZE6 has inhibited the denaturing of BSA at about 78–83%, therefore they were further evaluated through *in vivo* bioactivities. Potency of ZE6 was greater than that of MT and ET during *in vivo* anti-inflammatory activity. Analgesic potency of NMs was much higher than that of drugs (ET and MT). On per weight basis, the antipyretic potency of the NMs was higher than drugs (ET and MT). The results of LD50 method of *in vivo* acute toxicity activity have placed the NMs in category 3. The conjugation of NMs was confirmed from different spectroscopic techniques.

Declaration of Competing Interest

The authors declare that they have no known competing financial interests or personal relationships that could have appeared to influence the work reported in this paper.

Acknowledgements

The authors would like to extend their sincere appreciation to the Researchers Supporting Project Number (RSP2022R410), King Saud University, Riyadh, Saudi Arabia.

Funding

Supported by Researchers Supporting Project Number (RSP2022R410), King Saud University, Riyadh, Saudi Arabia.

References

Abbah, J., Amos, S., Chindo, B., Ngazal, I., Vongtau, H.O., Adzu, B., Farida, T., Odutola, A.A., Wambebe, C., Gamaniel, K.S., 2010. Pharmacological evidence favouring the use of Nauclea latifolia in malaria ethnopharmacy: effects against nociception, inflammation, and pyrexia in rats and mice. J. Ethnopharmacol. 127, 85–90.

Alvarenga, F.Q., Mota, B.C.F., Leite, M.N., Fonseca, J.M.S., Oliveira, D.A., de Andrade Royo, V., e Silva, M.L.A., Esperandim, V., Borges, A., Laurentiz, R.S., 2013. In vivo analgesic activity, toxicity and phytochemical screening of the hydroalcoholic extract from the leaves of Psidium cattleianum Sabine. J. Ethnopharmacol. 150, 280–284.

Azeem, A.K., Dilip, C., Prasanth, S.S., Shahima, V.J.H., Sajeev, K., Naseera, C., 2010. Anti–inflammatory activity of the glandular extracts of Thunnus alalunga. Asian Pac. J. Trop. Med. 3 (10), 794–796.

Aziz, M.A., Mehedi, M., Akter, M.I., Sajon, S.R., Mazumder, K., Rana, M.S., 2019. In vivo and in silico evaluation of analgesic activity of Lippia alba. Clin. Phytosci. 5, 1–9.

Bailey-Shaw, Y.A., Williams, L.A., Green, C.E., Rodney, S., Smith, A.M., 2017. In-vitro evaluation of the anti-inflammatory potential of selected Jamaican plant extracts using the bovine serum albumin protein denaturation assay. Int. J. Pharm. Sci. Rev. Res. 47, 145–153.

Cacciari, R.D., Menis, F., Biondi, M.A., Reynoso, E., Sabini, C., Montejano, H.A., Biasutti, M.A., 2020. Mechanistic analysis on the photochemistry of the anti-inflammatory drug etoricoxib in aqueous solution. Cytotoxicity of photoproducts. J. Photochem. Photobiol. A: Chem. 390, 112331.

Chandra, S., Chatterjee, P., Dey, P., Bhattacharya, S., 2012. Evaluation of in vitro anti-inflammatory activity of coffee against the denaturation of protein. Asian Pac. J. Tropical Biomed. 2 (1), S178–S180.

Crupi, R., Cuzzocrea, S., 2022. Role of EPA in inflammation: mechanisms, effects, and clinical relevance. Biomolecules 12, 242.

Das, A., Nayak, A.K., Mohanty, B., Panda, S., 2011. Solubility and dissolution enhancement of etoricoxib by solid dispersion technique using sugar carriers. ISRN Pharm. 2011, 1–8.
Karadağ, A.E., Demirci, F., Biltekin, S.N., Demirci, B., 2021. In vitro ACE2 and 5-LOX inhibition of Rosmarinus officinalis L. essential oil and its major component 1,8-cineole. Rec. Nat. Prod. (2), 194–199
Díaz-González, F., Sánchez-Madrid, F., 2015. NSAIDs: learning new tricks from old drugs. Eur. J. Immunol. 45 (3), 679–686.
Domper Arnal, M.-J., Hijos-Mallada, G., Lanas, A., 2021. Gastrointestinal and cardiovascular adverse events associated with NSAIDs. Expert Opin. Drug Saf., 1–12
El-Mekkawy, S., Shahat, A.A., Alqahtani, A.S., Alsaid, M.S., Abdelfattah, M.A., Ullah, R., Emam, M., Yasri, A., Sobeh, M., 2020. A Polyphenols-rich extract from moricandia sinaica boiss. Exhibits analgesic, anti-inflammatory and antipyretic activities in vivo. Molecules 25 (21), 5049.
Estella, O.U., William, A.C., Patrick, O., Ikenna, C., Mba, T., Obinna, O., Ginikachukwu, U., 2022. Evaluation of the analgesic and antipyretic activity of methanol extract of Combretum bauchiense Hutch & Dalziel (Combretaceae) leaves. Phytomed. Plus 2, 100166.
Fakhar-e-Alam, M., Rahim, S., Atif, M., Aziz, M.H., Malick, M.I., Zaidi, S., Suleman, R., Majid, A., 2013. ZnO nanoparticles as drug delivery agent for photodynamic therapy. Laser Phys. Lett. 11, 025601.
Gaihre, B., Khil, M., Lee, D., Kim, H., 2009. Gelatin-coated magnetic iron oxide nanoparticles as carrier system: drug loading and in vitro drug release study. Int. J. Pharm. 365 (1-2), 180–189.
Ghorbani, H., Mehr, F., Pazoki, H., Rahmani, B., 2015. Synthesis of ZnO nanoparticles by precipitation method. Orient. J. Chem. 31 (2), 1219–1221.
Gupta, S., Mishra, K., Gupta, R., Singh, S., 2021. Andrographolide–A prospective remedy for chikungunya fever and viral arthritis. Int. Immunopharmacol. 99, 108045.
Guvenal, T., Yanar, O., Timuroglu, Y., Cetin, M., Cetin, A., 2021. Effects of selective and non-selective cyclooxygenase (COX) inhibitors on postoperative adhesion formation in a rat uterine horn model. Clin. Exp. Obstet. Gynecol. 37, 49–52.
Hameed, H.A., Khan, S., Shahid, M., Ullah, R., Bari, A., Ali, S.S., Hussain, Z., Sohail, M., Khan, S.U., Htar, T.T., 2020. Engineering of naproxen loaded polymer hybrid enteric microspheres for modified release tablets: development, characterization, in silico modelling and in vivo evaluation. Drug Design Dev. Ther. 14, 27.
Harb, H., Benamar, M., Lai, P.S., Contini, P., Griffith, J.W., Crestani, E., Schmitz-Abe, K., Chen, Q., Fong, J., Marri, L., 2021. Notch4 signaling limits regulatory T-cell-mediated tissue repair and promotes severe lung inflammation in viral infections. Immunity 54, 1186-1199. e1187.
Hassan, F.I., Zezi, A.U., Yaro, A.H., Danmalam, U.H., 2015. Analgesic, anti-inflammatory and antipyretic activities of the methanol leaf extract of Dalbergia saxatilis Hook. F in rats and mice. J. Ethnopharmacol. 166, 74–78.
Ilavarasan, R., Mallika, M., Venkataraman, S., 2006. Anti-inflammatory and free radical scavenging activity of Ricinus communis root extract. J. Ethnopharmacol. 103 (3), 478–480.
Janani, B., Syed, A., Raju, L.L., Al-Harthi, H.F., Thomas, A.M., Das, A., Khan, S.S., 2020. Synthesis of carbon stabilized zinc oxide nanoparticles and evaluation of its photocatalytic, antibacterial and anti-biofilm activities. J. Inorg. Organomet. Polym Mater. 30 (6), 2279–2288.
Jat, R., Chhipa, R., Sharma, S., 2010. Spectrophotometric quantification of Etoricoxib in bulk drug and tablets using hydrotropic agent. Pharmacophore 1, 96–102.
Jiang, Q., Im, S., Wagner, J.G., Hernandez, M.L., Peden, D.B., 2022. Gamma-tocopherol, a major form of vitamin E in diets: Insights into antioxidant and anti-inflammatory effects, mechanisms, and roles in disease management. Free Radical Biol. Med. 178, 347–359.
Kaduševičius, E., 2021. Novel applications of NSAIDs: Insight and future perspectives in cardiovascular, neurodegenerative, diabetes and cancer disease therapy. Int. J. Mol. Sci. 22, 6637.
Kesharwani, R., Sachan, A., Singh, S., Patel, D., 2016. Formulation and evaluation of solid lipid nanoparticle (SLN) based topical gel of etoricoxib. J. Appl. Pharm. Sci. 6, 124–131.
Kolhe, A., Kale, A., 2017. Evaluation of analgesic, anti-inflammatory, and antipyretic activity of leukotriene receptor antagonist-montelukast: An experimental study. Natl. J. Physiol. Pharm. Pharmacol. 7 (1), 32.
Kwiecien, S.Y., McHugh, M.P., 2021. The cold truth: the role of cryotherapy in the treatment of injury and recovery from exercise. Eur. J. Appl. Physiol. 121 (8), 2125–2142.
Leelaprakash, G., Dass, S.M., 2011. Invitro anti-inflammatory activity of methanol extract of Enicostemma axillare. Int. J. Drug Dev. Res. 3, 189–196.
Liu, N., Bai, L., Lu, Z., Gu, R., Zhao, D., Yan, F., Bai, J., 2022. TRPV4 contributes to ER stress and inflammation: implications for Parkinson's disease. J. Neuroinflamm. 19, 1–15.
Luna, I.Z., Hilary, L.N., Chowdhury, A.M.S., Gafur, M.A., Khan, N., Khan, R.A., 2015. Preparation and characterization of copper oxide nanoparticles synthesized via chemical precipitation method. Open Access Libr. J. 02 (03), 1–8.
Makonnen, E., Debella, A., Zerihun, L., Abebe, D., Teka, F., 2003. Antipyretic properties of the aqueous and ethanol extracts of the leaves of Ocimum suave and Ocimum lamiifolium in mice. J. Ethnopharmacol. 88 (1), 85–91.
Moilanen, L.J., Laavola, M., Kukkonen, M., Korhonen, R., Leppänen, T., Högestätt, E.D., Zygmunt, P.M., Nieminen, R.M., Moilanen, E., 2012. TRPA1 contributes to the acute inflammatory response and mediates carrageenan-induced paw edema in the mouse. Sci. Rep. 2, 1–6.
Moore, N., Pollack, C., Butkerait, P., 2015. Adverse drug reactions and drug–drug interactions with over-the-counter NSAIDs. Ther. Clin. Risk Manag. 11, 1061.
O'Callaghan, J.P., Holtzman, S.G., 1975. Quantification of the analgesic activity of narcotic antagonists by a modified hot-plate procedure. J. Pharmacol. Exp. Ther. 192, 497–505.
Parra, A.L., Yhebra, R.S., Sardiñas, I.G., Buela, L.I., 2001. Comparative study of the assay of Artemia salina L. and the estimate of the medium lethal dose (LD50 value) in mice, to determine oral acute toxicity of plant extracts. Phytomedicine 8, 395–400.
Patel, H., Suhagia, B., Shah, S., Rathod, I., Parmar, V., 2007. Preparation and characterization of etoricoxib-β-cyclodextrin complexes prepared by the kneading method. Acta Pharm. 57, 351–359.
Pathak, A.K., Argal, A., 2007. Analgesic activity of Calotropis gigantea flower. Fitoterapia 78 (1), 40–42.
Patil, B.N., Taranath, T.C., 2016. Limonia acidissima L. leaf mediated synthesis of zinc oxide nanoparticles: a potent tool against Mycobacterium tuberculosis. Int. J. Mycobacteriol. 5 (2), 197–204.
Pawlosky, N., 2013. Cardiovascular risk: Are all NSAIDs alike? Can. Pharm. J./Revue des Pharmaciens du Canada 146 (2), 80–83.
Pohocha, N., Grampurohit, N.D., 2001. Antispasmodic activity of the fruits of Helicteres isora Linn. Phytother. Res. 15 (1), 49–52.
Prabhu, Y.T., Rao, K.V., Kumar, V.S.S., Kumari, B.S., 2013. Synthesis of ZnO nanoparticles by a novel surfactant assisted amine combustion method. Adv. Nanopart. 02 (01), 45–50.
Prajapati, M., Yamgar, D.B., Desale, M.N., Fegade, B., 2022. A Review on Various Analytical Methodologies for Etoricoxib. Adv. J. Grad. Res. 11, 61–70.
Priyanka, K., Abdul Hasan, S.A., 2012. Preparation and evaluation of montelukast sodium loaded solid lipid nanoparticles. J. Young Pharm. 4 (3), 129–137.
Rahmawati, L., Park, S.H., Kim, D.S., Lee, H.P., Aziz, N., Lee, C.Y., Kim, S.A., Jang, S.G., Kim, D.S., Cho, J.Y., 2022. Anti-inflammatory activities of the ethanol extract of Prasiola japonica, an edible freshwater green algae, and its various solvent fractions in LPS-induced macrophages and carrageenan-induced paw edema via the AP-1 pathway. Molecules 27, 194.
Raoufi, D., 2013. Synthesis and microstructural properties of ZnO nanoparticles prepared by precipitation method. Renewable Energy 50, 932–937.
Ratheesh, M., Helen, A., 2007. Anti-inflammatory activity of Ruta graveolens Linn on carrageenan induced paw edema in wistar male rats. Afr. J. Biotechnol. 6.
Romadhan, M.F., Suyatma, N.E., Taqi, F.M., 2016. Synthesis of ZnO nanoparticles by precipitation method with their antibacterial effect. Indonesian J. Chem. 16, 117–123.
Sağlık, B.N., Osmaniye, D., Levent, S., Çevik, U.A., Çavuşoğlu, B.K., Özkay, Y., Kaplancıklı, Z.A., 2021. Design, synthesis and biological assessment of new selective COX-2 inhibitors including methyl sulfonyl moiety. Eur. J. Med. Chem. 209, 112918.
Saleem, TK.M., Azeem, A.K., Dilip, C., Sankar, C., Prasanth, N.V., Duraisami, R., 2011. Anti-inflammatory activity of the leaf extracts of Gendarussa vulgaris Nees. Asian Pac. J. Trop. Biomed. 1 (2), 147–149.
Saravanan, M., Gopinath, V., Chaurasia, M.K., Syed, A., Ameen, F., Purushothaman, N., 2018. Green synthesis of anisotropic zinc oxide nanoparticles with antibacterial and cytofriendly properties. Microb. Pathog. 115, 57–63.
Saravanan, M., Siva kumari, K., Pratap Reddy, P., Naidu, M.N., Moses Babu, J., Srivastava, A.K., Lakshmi Kumar, T., Chandra Sekhar, B.V.V.N., Satyanarayana, B., 2008. Identification, synthesis, isolation and spectral characterization of potential impurities of montelukast sodium. J. Pharm. Biomed. Anal. 48 (3), 708–715.
Senthilkumar, K., Vijaya, C., 2015. Formulation development of mouth dissolving film of etoricoxib for pain management. Adv. Pharm. 2015, 1–11.
Sharma, D., Sharma, S., Kaith, B.S., Rajput, J., Kaur, M., 2011. Synthesis of ZnO nanoparticles using surfactant free in-air and microwave method. Appl. Surf. Sci. 257 (22), 9661–9672.
Singh, A., 2022. Evaluation of Pharmacological Effect of Cassia Sophera Linn leaves extracts. J. Appl. Pharm. Sci. Res. 4, 29–32.
Singh, S., Mishra, A., Verma, A., Ghosh, A.K., Mishra, A.K., 2012. A simple Ultraviolet spectrophotometric method for the determination of etoricoxib in dosage formulations. J. Adv. Pharm. Technol. Res. 3 (4), 237.
Singh, S.P., Ankesh Kumar, A., Bhavsar, P., Bhavsar, M., Sourya, N., Singh, A.K., Sahu, M., 2021. Application of non-steroidal anti-inflammatory drugs (NSAIDs) for improvement of cattle fertility. Pharma Innovat. 10, 404–407.
Sinha, M., Gautam, L., Shukla, P.K., Kaur, P., Sharma, S., Singh, T.P., 2013. Current perspectives in NSAID-induced gastropathy. Mediators Inflamm., 1–11
Sinniah, A., Yazid, S., Flower, R.J., 2021. From NSAIDs to glucocorticoids and beyond. Cells 10, 3524.
Syed, A., Al Saedi, M.H., Bahkali, A.H., Elgorban, A.M., Kharat, M., Pai, K., Ghodake, G., Ahmad, A., 2021. Biological synthesis of α-Ag2S composite nanoparticles using the fungus Humicola sp. and its biomedical applications. J. Drug Deliv. Sci. Technol. 66, 102770.
Syed, A., Al Saedi, M.H., Bahkali, A.H., Elgorgan, A.M., Kharat, M., Pai, K., Pichtel, J., Ahmad, A., 2022. αAu2S nanoparticles: Fungal-mediated synthesis, structural characterization and bioassay. Green Chem. Lett. Rev. 15 (1), 59–68.
Syed, A., Saraswati, S., Kundu, G.C., Ahmad, A., 2013. Biological synthesis of silver nanoparticles using the fungus Humicola sp. and evaluation of their cytotoxicity using normal and cancer cell lines. Spectrochim. Acta Part A Mol. Biomol. Spectrosc. 114, 144–147.
Ullah, R., Alsaid, M.S., Alqahtani, A.S., Shahat, A.A., Naser, A.A., Mahmood, H.M., Ahamad, S.R., Al-Mishari, A.A., Ahmad, S., 2019. Anti-inflammatory, antipyretic,

analgesic, and antioxidant activities of Haloxylon salicornicum aqueous fraction. Open Chem. 17 (1), 1034–1042.
Vane, J.R., Botting, R.M., 1996. Mechanism of action of anti-inflammatory drugs. Scand. J. Rheumatol. 25 (sup102), 9–21.
Sridhar, B.K., Shivakumar, S., Wahid, A., 2008. Preparation and evaluation of transdermal drug delivery system of etoricoxib using modified chitosan. Indian J. Pharm. Sci. 70 (4), 455.
Walia, V., Thakur, S., 2021. Role of NSAIDs in cancer prevention and cancer promotion. J. Can. Sci. Res. 6, 119.
Williams, L., O'Connar, A., Latore, L., Dennis, O., Ringer, S., Whittaker, J., Conrad, J., Vogler, B., Rosner, H., Kraus, W., 2008. The in vitro anti-denaturation effects induced by natural products and non-steroidal compounds in heat treated (immunogenic) bovine serum albumin is proposed as a screening assay for the detection of anti-inflammatory compounds, without the use of animals, in the early stages of the drug discovery process. West Indian Med. J. 57, 327–331.
Xiong, H.-M., 2013. ZnO nanoparticles applied to bioimaging and drug delivery. Adv. Mater. 25 (37), 5329–5335.
Yedurkar, S., Maurya, C., Mahanwar, P., 2016. Biosynthesis of zinc oxide nanoparticles using Ixora coccinea leaf extract—a green approach. Open J. Synth. Theor. Appl. 5, 1.
Zhang, Y.-Y., Huang, Y.-F., Liang, J., Zhou, H., 2022. Improved up-and-down procedure for acute toxicity measurement with reliable LD50 verified by typical toxic alkaloids and modified Karber method. BMC Pharmacol. Toxicol. 23, 1–11.
Zhou, Y., Khan, H., Xiao, J., Cheang, W.S., 2021. Effects of arachidonic acid metabolites on cardiovascular health and disease. Int. J. Mol. Sci. 22, 12029.